Int. J. Heat Mass Transfer. Vol. 36, No. 16, pp. 3975–3982, 1993
Printed in Great Britain

0017–9310/93 $6.00+0.00

Comparison of engineering models of nongray behavior of combustion products

TAE-HO SONG

Department of Mechanical Engineering, Korea Advanced Institute of Science and Technology, Kusong-dong 400, Yusong-ku, Taejon, Korea

(*Received* 8 *January* 1993 *and in final form* 15 *April* 1993)

Abstract—Various engineering models of nongray behavior of combustion products are compared with one another for two types of sample problem. The Curtis–Godson approximation method and the weighted-sum-of-gray-gases-model (WSGGM) are used to compute the emission from a Lorentz line in a non-isothermal path, as the first problem. The Milne–Eddington type WSGGM underestimates the effective line width. Secondly, the gray gas model, the WSGGM and the spectral group model (SGM, a modification of WSGGM) are used to solve one-dimensional inhomogeneous slab problems and are compared with the nongray wide band results. The results from both the WSGGM and the SGM are in good agreement with the reference. The result from the gray gas model is significantly away from those of the other models.

INTRODUCTION

SPECTRALLY complicated behavior of combustion gas radiation has been imposing challenging problems to heat transfer engineers. A great deal of effort has been exercised to accurately model the nongray behavior of typical combustion products such as H_2O and CO_2.

The commonly used gray gas model may give erroneous results when applied to enclosures filled with combustion gas, while the WSGGM has been developed for engineering problems of heat transfer predictions [1]. Smith and his coworkers [2] tabulated the regression coefficients for the weighting factors of the gray gases for combustion products, while Modest [3] used the model parameters to calculate the heat transfer in many situations for a wide band. A similar model to WSGGM was developed to predict the spectral behavior in a more realistic manner by explicitly specifying the spectral interval for each individual gray gas [4]. It was named the spectral group model (SGM). They applied this model to Grosshandler's flame data [5] and good agreement was observed. The success of narrow band model [6] was followed by the wide band model [7, 8]. Both were highly accurate and reliable. For inhomogeneous medium, the Curtis–Godson approximation [9] was applied to the narrow band model [6] as well as to the wide band model to give fairly accurate results [10, 11]. Accuracy of the Curtis–Godson approximation was improved by Lindquist and Simmons [12]. The wide band model was applied to coal-fired furnaces by Menguc and Viskanta [13] by assuming partly gray behavior around the centers of the wide bands. Grosshandler [5] investigated the problem of radiative heat transfer by examining the equivalent transmittance. He treated the whole spectrum as a region of some transmittance. Zhang *et al.* [14] pointed out that the correlation between the intensity and the spectral transmittance was very important even for a narrow band. The computational results of Kim *et al.* [15] confirmed that the computational results could be qualitatively wrong when the correlation term was neglected. They concluded that both of the nongray narrow and wide band models were accurate ('nongray' means that the correlation is considered).

Although there are many engineering models of nongray behavior of combustion gases, none of them are perfect for applications. The criteria for a good engineering model could be set as follows: (i) it should be easy to incorporate with any radiation solvers, (ii) it can be extended further to any degree of modeling accuracy and (iii) the computing time should be reasonable. The narrow band model is accurate even when the Curtis–Godson approximation is used for nonuniform gas layer. However, it is not easily combined with the radiation solvers except with the discrete ordinate method, and the computation of correlation requires rather excessive computing time and effort [15]. While the wide band model has similar characteristics, it can be incorporated with other radiation solvers if partly gray behavior is assumed as Menguc and Viskanta have done in their work [13]. In their work, the correlation between the intensity and the spectral transmittance was neglected [15]. The WSGGM is most convenient to combine with any radiation solver with a reasonable computing time. However, the detailed information of spectral behavior is lost and no critical examination of the validity of this model for inhomogeneous layers of combustion gases has been made. The SGM reveals the spectral behavior of the radiation to a certain degree, and it can be further extended to any degree of accuracy. Although it certainly covers the shortcomings of the WSGGM, it has never been thoroughly checked for more general cases.

It is the aim of this paper to compare the gray gas

NOMENCLATURE

a	line parameter, γ/δ	γ	line half width
A	effective width	δ	line spacing
E	modeling error	ε	gas emissivity
E_b	blackbody emissive power	η	wavenumber
E_n	exponential integral function	κ	absorption coefficient
F	total radiative heat flux	τ	optical depth
g	normalized shape of the line	τ_t	transmittance.
I	radiation intensity		
L	length of the path, or the 1-D layer	Subscripts	
M	number of spectral groups or gray gases	b	blackbody
s	coordinate along the radiation path	c	at the line center
S	integrated absorption coefficient of a line	e	equivalent parameters of Curtis–Godson approximation
T	temperature		
W	weighting factor	j	index of gray gas or spectral group
x	dimensionless optical path, $SL/2\pi\gamma$	l	line
z	coordinate in the 1-D layer.	m	modeled value
		o	reference value
Greek symbols		t	true value
α	Milne–Eddington wavenumber function	w	at wall
β	Milne–Eddington path function	η	at a wavenumber.

model, the WSGGM, the Curtis–Godson approximation, the nongray wide band model and the SGM applied to two types of problem. First, emission from a Lorentz line or a group of isolated lines in a nonuniform layer is calculated using the WSGGM and the Curtis–Godson approximation. The results are examined with exact solution. Secondly, a one-dimensional slab layer problem with various temperature distribution is solved using gray gas model, WSGGM and SGM and the results are compared with the nongray wide band solutions of Kim *et al.* [15] based on the method of Zhang *et al.* [14].

EMISSION FROM A LORENTZ LINE IN A NONISOTHERMAL LAYER

A limiting case of gas radiation is the emission from a group of isolated lines. In this limit, each line behaves in an independent manner. Therefore the overall modeling is accurate if each single line is accurately modeled. Indeed, the elaborate modeling of a single line may not be very meaningful for practical applications. However, it is helpful in critically examining the validity of the models. The line emission from a layer of gas is expressed as an effective line width A_l. The effective line width for a single line can be obtained analytically when the gas is homogeneous [6]. However, numerical integration or the Curtis–Godson approximation or similar ones need be made when the gas is inhomogeneous. The numerical integration is carried out for inhomogeneous path of length L by direct integration of the spectral intensity at L over all the wavenumber η, i.e.

$$A_l(L) = \int_{\eta=0}^{\infty} \int_{s=0}^{L} \kappa_\eta(s) \frac{I_{b\eta}(s)}{I_{bo}} \times \left[\exp\left(- \int_s^L \kappa_\eta(s') \, ds' \right) \right] ds \, d\eta \quad (1)$$

where the spectral blackbody intensity $I_{b\eta}$ is scaled to a reference value I_{bo}.

Collision broadening is the major line broadening mechanism in many combustion facilities. The line shape is a Lorentz profile whose half width is inversely proportional to the temperature. In this paper, the Lorentz profile with variable half width is used. Then the line shape is expressed as

$$\kappa_\eta = \kappa_c(s) g\left(\frac{|\eta - \eta_c|}{\gamma(s)} \right) \quad (2)$$

where $\kappa_c(s)$ is the absorption coefficient at the line center, γ the line half width and $g(\eta^*)$ the Lorentz profile normalized with $\kappa_c(s)$.

$$g(\eta^*) = \frac{1}{1+\eta^{*2}}. \quad (3)$$

The optical depth τ is defined as $\kappa_c s$ and it is assumed that κ_c is constant everywhere. The temperature is assumed to vary linearly along s from zero. Then the collision half width is given as

$$\frac{\gamma(s)}{\gamma_o} = \left(\frac{s}{L} \right)^{1/2}. \quad (4)$$

Also, it is assumed that the Rayleigh–Jeans formula is applicable. This means that the spectral blackbody

intensity is proportional to the temperature. Thus, with $I_{bo} = I_{b\eta}(L)$,

$$\frac{I_{b\eta}(s)}{I_{bo}} = \frac{s}{L}. \tag{5}$$

Note that once the temperature is determined, the spectral variation of blackbody intensity in the line is neglected. After a tedious mathematical manipulation, the line width at length L is nondimensionalized by γ_o and is given by

$$\frac{A_l(L)}{\gamma_o} = 2\tau_L \int_{\eta^*=0}^{\infty} \int_{\tau^*=0}^{1.0} \tau^* \left(\frac{1+\eta^{*2}}{1+\eta^{*2}\tau^*}\right)^{-\tau_L/\eta^{*2}} \times \frac{1}{1+\eta^{*2}\tau^*} d\tau^* d\eta^* \tag{6}$$

where $\tau_L = \kappa_c L$. A similar derivation for the effective line width at $\tau = 0$ (this means the radiation from the layer to the plane $s = 0$) leads to

$$\frac{A_l(0)}{\gamma_o} = 2\tau_L \int_{\eta^*=0}^{\infty} \int_{\tau^*=0}^{1.0} \tau^*(1+\eta^{*2}\tau^*)^{-\tau_L/\eta^{*2}} \times \frac{1}{1+\eta^{*2}\tau^*} d\tau^* d\eta^*. \tag{7}$$

Meanwhile, the effective line width for a homogeneous layer is given as [6]

$$A_l = 2\pi\gamma x e^{-x}[I_o(x)+I_1(x)] \tag{8}$$

where $x = SL/2\pi\gamma$, s the integrated absorption coefficient and I_n the modified Bessel function of the first kind, of order n. Using two parameters $\bar{\kappa}(=S/\delta)$ and $a(=\gamma/\delta)$, the above equation is rewritten as

$$\frac{A_l}{\delta} = 2\pi a f\left(\frac{L\bar{\kappa}}{2\pi a}\right) \tag{9}$$

where $f(x) = xe^{-x}[I_o(x)+I_1(x)]$. The two parameters $\bar{\kappa}$ and a are replaced by equivalent parameters $\bar{\kappa}_e$ and a_e for a nonuniform layer in the Curtis–Godson approximation and the effective line width is denoted as $A_l(0 \to L)$. Note that the fictitious line spacing δ is constant.

$$\bar{\kappa}_e(0 \to L) = \frac{1}{L}\int_0^L \bar{\kappa}(s)\, ds \tag{10}$$

$$a_e(0 \to L) = \frac{1}{\bar{\kappa}_e L}\int_0^L a(s)\bar{\kappa}(s)\, ds. \tag{11}$$

Since the gas-emitted spectral intensity I_η at L is

$$I_\eta(L) = \int_0^L I_{b\eta}(s)\frac{\partial\tau_t(s \to L)}{\partial s} ds \tag{12}$$

where $\tau_t(s \to L)$ is the transmittance between s and L. The above equation is integrated over a wavenumber interval δ and it is divided by I_{bo}. The result is an approximated value of $A_l(L)$. Using the relation $\tau_t(s \to L) = 1 - A_l(s \to L)/\delta$, $A_l(L)$ can be expressed as

$$A_l(L) \approx \int_0^L A_l(s \to L)\, d\left(\frac{s}{L}\right). \tag{13}$$

Similarly, the effective line width at $s = 0$ is (also normalized by I_{bo}) given as

$$A_l(0) \approx A_l(0 \to L) - \int_0^L A_l(0 \to s)\, d\left(\frac{s}{L}\right). \tag{14}$$

Evaluation of equation (13) requires numerical computation. However, the right hand side of equation (14) can be obtained algebraically since $a_e(0 \to x)$ approaches infinity and an asymptotic formula can be used for the modified Bessel functions of the first kind

$$A_l(0) \approx \frac{2\pi\gamma_o}{3}\tau_L. \tag{15}$$

On the other hand, the WSGGM, when applied to the total spectrum, decides the weights of gray portion to the total blackbody emissive power. When it is applied to a spectral line, it determines the wavenumber width of the gray portion instead of the weight. This process is schematically shown by the histogram of Fig. 1(a). Modest [3] calculated the band absorptances of the gray portions for a wide band with a fixed band width. In this paper, attention is paid to the case where the half width varies although the line shape remains the same. A possible way to handle this case is to decide the nondimensional width of each gray portion (width divided by the line half width). It then results in the same nondimensional width as well as the same dimensionless absorption coefficient (the gray absorption coefficient divided by the line center

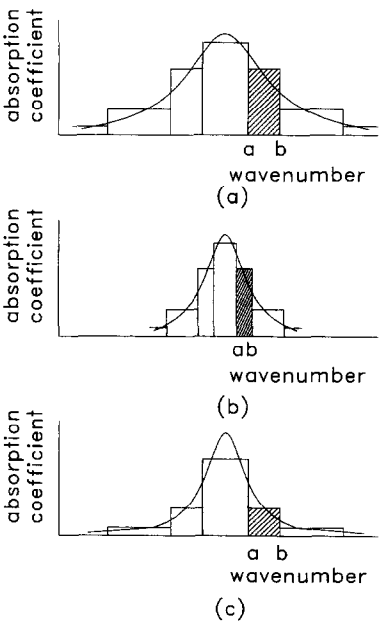

FIG. 1. Modeling of a single line with variable half width using the Milne–Eddington type WSGGM ((a) and (b)) and SGM ((a) and (c)). The line shapes in (b) and (c) are identical with each other and are contracted horizontally from (a).

absorption coefficient). This practice is shown in Fig. 1(b). The gray gas portion (see the hatched histograms) is either contracted or expanded at a different line width. To calculate the radiation transfer along a path of line shape variation, the radiative transfer equation (RTE) in a nonscattering medium is integrated over a gray gas portion to give

$$\frac{\partial}{\partial s}\int_a^b I_\eta(s)\,d\eta = -\bar{\kappa}\int_a^b I_\eta(s)\,d\eta + \bar{\kappa}\int_a^b I_{b\eta}\,d\eta + \frac{\partial b}{\partial s}I_\eta(b) - \frac{\partial a}{\partial s}I_\eta(a) \quad (16)$$

where $\bar{\kappa}$ is the mean absorption coefficient over the interval (a, b). The last two terms in the right hand side are due to the Leibnitz rule and are very difficult to estimate. If it is neglected, the modeling process becomes a Milne–Eddington type modeling, $\kappa_\eta(T, P) = \alpha(\eta)\beta(T, P)$. This is named a Milne–Eddington type WSGGM. In another practice, when the wavenumber boundaries a and b are fixed (see Fig. 1(c)), these terms disappear. As the number of gray gas is increased infinitely, the result becomes exact as given by equations (6) and (7). To fix the wavenumber boundaries of a gray portion is the basic idea of the SGM and thus it is also named SGM here too.

The error of Milne–Eddington type WSGGM is calculated when the number of gray portion is increased infinitely.

$$\frac{A_1(L)}{\gamma_0} \approx 2\tau_L\int_{\eta^*=0}^{\infty}\int_{\tau^*=0}^{1.0}\tau^*\exp\left[\frac{\tau_L}{1+\tau^{*2}}(\tau^*-1)\right]\times\frac{1}{1+\eta^{*2}}\,d\tau^*\,d\eta^* \quad (17)$$

$$\frac{A_1(0)}{\gamma_0} \approx 2\tau_L\int_{\eta^*=0}^{\infty}\int_{\tau^*=0}^{1.0}\tau^*\exp\left[-\frac{\tau_L}{1+\tau^{*2}}\tau^*\right]\times\frac{1}{1+\eta^{*2}}\,d\tau^*\,d\eta^*. \quad (18)$$

The computational results are shown in Fig. 2. In general, the Milne–Eddington type WSGGM results show smaller effective line width. The difference is very small at $s = 0$ for very large optical depths. In all other cases, the difference is as large as 25%. The Milne–Eddington type WSGGM always underestimates the effective line width. It is analogous to the findings of Felske and Tien [16] who have shown that the Milne–Eddington behavior underestimates the effective band width for an exponential wide band in their tested cases. This result confirms that the Milne–Eddington type WSGGM has fundamental limitation in predicting the line emission correctly. The Curtis–Godson approximation is erroneous in the prediction of $A_1(0)$ when the optical thickness is large. This error is caused by the increase of the parameter $a_e(0 \to x)$ to infinity. In other predictions, it is close to the exact results.

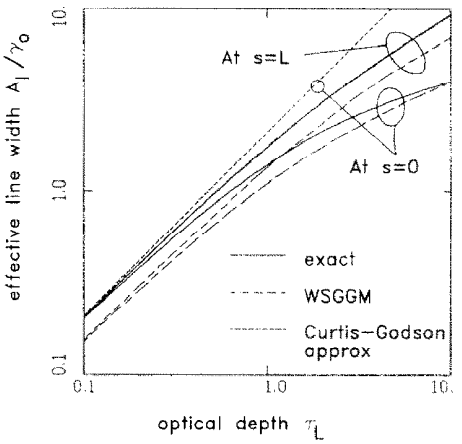

FIG. 2. Prediction of the effective line width of the single line with Lorentz profile and linear temperature variation with the optical depth τ when using the Curtis–Godson approximation and the Milne–Eddington type WSGGM with infinite number of gray gases. At $s = L$, the Curtis–Godson approximation is nearly exact.

THE 1-D INHOMOGENEOUS LAYER

In this section, the whole spectrum is considered for the accurate prediction of total intensity in a layer of inhomogeneous gas.

As the test problems, those of Kim *et al.* [15] are chosen. They presented elaborate computational results for layers of known temperature distribution (uniform, parabolic and boundary layer type) and H_2O concentration distribution where the water vapor was the only radiation emitter/absorber in a total pressure of 1 atm. The heat source strength distribution in the medium and the wall heat flux were obtained using correlated/noncorrelated and narrow/wide band models. They used the S_{20} method so that the error due to the inaccuracy of the RTE approximation was negligible, and the Curtis–Godson approximation they used was not considered to have induced significant error for the given temperature variation [17]. They showed that the partly gray assumption in a certain wavenumber interval could lead to large error depending on the problems. As has been previously shown by Zhang *et al.* [14] and Nelson [18], the 'nongray' computation including the intensity–transmittance correlation is highly accurate, whether the wide or the narrow band is used. Spectral group modeling is devised in this study using the wide band model of Edwards [7]. This is the same model as used by Kim *et al.* [15] in the above study and at the same time, by Smith *et al.* [2] for a WSGGM for water vapor. To be consistent with each other, the nongray wide band results of Kim *et al.* [15] are used as the benchmark solutions in this analysis.

The water vapor was modeled by Smith *et al.* [2] in a 4 WSGGM (4 gray gases) which included the transparent window. The average modeling error of the gas emissivity was 5–6% in the region of temperature from 300 to 1500 K and length from 0.01 to

5 m at 1 atm. Application of WSGGM to inhomogeneous layer is made here by integrating the RTE over the gray gas wavenumber intervals as given by equation (16). Since no information on the change of wavenumber intervals is given by the WSGGM, the last two terms are neglected. The gray gas portion with the highest absorption coefficient at a temperature is identified with the one with the highest absorption coefficient at another temperature in evaluating equation (16) (see Figs. 1(a) and (b)). Those with the second highest absorption coefficient at various temperatures are a gray gas portion too. This identification of gray gas portions persists to the most transparent one.

The spectral group modeling was introduced to fix the wavenumber intervals of the gray portions at any temperature. In this case the last two terms of equation (16) disappear automatically. The wide band model of Edwards [7] is incorporated in this modeling. The SGM is similar to the WSGGM except that the SGM decides the wavenumber intervals of each gray gas located around the center of each wide band, while the WSGGM decides the weights directly. The SGM error of emissivity is minimized, i.e.

$$\min E = \sum_T \sum_L \left(\frac{\varepsilon_m}{\varepsilon_t} - 1 \right)^2 \tag{19}$$

where the model emissivity is expressed as

$$\varepsilon_m(T, L) = \sum_j^M (1 - e^{-\kappa_j L}) W_j(T). \tag{20}$$

The weight of the jth spectral group W_j is computed by adding the spectral blackbody intensity at each band center multiplied by the wavenumber interval and dividing by the total blackbody intensity. It is thus a function of temperature. The most transparent spectral group is numbered last, i.e. $j = M$. This group occupies the wavenumber region not occupied by the other spectral groups, which means that its weight is 1 minus the weights of the other spectral groups. Although it is a common practice in the WSGGM to assign zero absorption coefficient to this group, it is not very necessary in general. Thus, some nonzero absorption coefficient is also assigned to this group. Note that the SGM is identical to the gray gas model if M is unity.

The 'true' emissivity ε_t is obtained using the wide band model of Edwards [7]. Around the following seven band centers, the wavenumber intervals for $j = 1, \ldots, M-1$ are optimally decided to minimize equation (19): 1600, 3760, 5350, 7250, 667, 2326, 3660 cm^{-1}. The minimization scheme is constructed by using a double loop of steepest descent method. In the outer loop, the wavenumber intervals for each of the spectral group around the above band centers are varied, which results in 7 times $M-1$ independent variables. In the inner loop, the M absorption coefficients are optimally decided at the given wavenumber intervals. In this loop, the absorption coefficient may or may not vary with temperature. The former gives better results. However, the latter is convenient to use and as accurate for most cases. The latter is practiced here. The test path lengths and temperatures are: $L = 0.02, 0.05, 0.1, 0.2, 0.5, 1.0, 2.0, 5.0$ m; $T = 300, 600, 900, 1200, 1500$ K. The modeled results for a gray gas model and 4 SGM (SGM with 4 gray gases) are as follows:

Gray gas model; 0.9097 m^{-1}

4 SGM; 32.75, 4.849, 0.9644, 0.0494 m^{-1}.

The average relative errors of modeling are 57 (gray gas model) and 6.13 (4 SGM) percent, respectively.

The problem of Kim *et al.* [15] can be solved exactly using the exponential integral function [19]. In this method, the radiative heat flux to the positive z-axis F is calculated first. The values of F at $z = 0$ and L give the wall heat flux and the derivative of F with the coordinate z is the strength of the heat source in the medium. The expression for F is given by Crosbie and Viskanta [20] for gray medium and it can be easily applied to the WSGGM or the SGM behavior of gases.

$$\begin{aligned} F(z) = 2\pi \sum_j^M \Big[& I_b(0) W_j(T_{w0}) E_3(\kappa_j z) \\ & + \int_0^z \kappa_j(z') I_b(z') W_j(z') E_2(\kappa_j z - \kappa_j z') \, dz' \\ & - I_b(L) W_j(T_{wL}) E_3(\kappa_j L - \kappa_j z) \\ & - \int_z^L \kappa_j(z') I_b(z') W_j(z') E_2(\kappa_j z' - \kappa_j z) \, dz' \Big] \end{aligned} \tag{21}$$

where T_{w0} and T_{wL} are the temperatures of the black walls at $z = 0$ and L, respectively, and E_n is the nth exponential integral function. A value of F is computed at every value of z and later, second order numerical differentiation is made to obtain the heat source strength.

The computational results are presented in Figs. 3–6. About 1% deviation is observed in the heat flux F depending on the numerical integration scheme used for the integrals in equation (21). A uniform distribution of the integrated function in a control volume is employed in this computation. Figure 3 shows the heat source distribution for the parabolic-type temperature distribution. The result from the gray gas computation shows very large deviation from that of the reference nongray wide band computation. The results of the WSGGM and the SGM are both in good agreement with that of the reference computation. In Fig. 4(a), results for water vapor layer of thickness 0.1 m, at uniform temperature of 1000 K, bounded by cold black walls are given. The solution from the gas model again shows large deviation from the reference while the results by WSGGM and SGM are in good agreement. The same conclusion is observed for

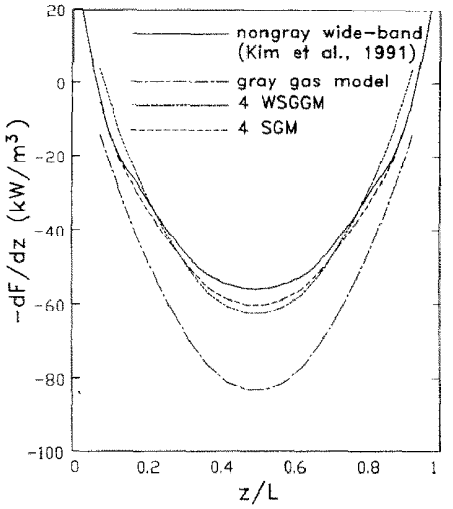

FIG. 3. The radiative source for parabolic temperature profile of Kim *et al.* [15]. (Center at 886 K and black boundaries at 400 K, layer depth = 0.4 m.)

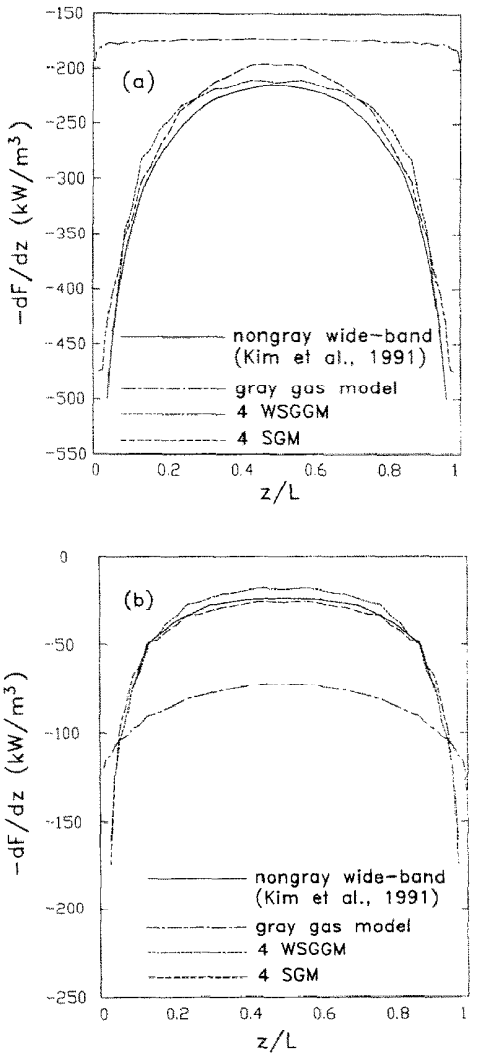

FIG. 4. The radiative source for uniform temperature profile of Kim *et al.* [15]. (Temperature: 1000 K with cold black walls, layer depth = 0.1 m (a) and 1.0 m (b).)

layer thickness of 1.0 m as depicted in Fig. 4(b). Note that the strength of heat source is smaller than before. The boundary layer type temperature profile as used in Fig. 5 has wall temperatures of 1500 K at $z = 0$ and 300 K at $z = 0.2$ m. The sudden temperature drop away from the wall is characterized by the spike in the graph. Again, the result of the gray gas model is far off from the reference, while the rest show reasonable agreement with the reference. The position of the peak value is well predicted by all these models, however, the peak value of the heat source is predicted smaller than the reference. In general, the gray gas model yields results with the deviation of 10–100% compared with the reference. The gray gas model may result in large error when applied to a highly inhomogeneous layer. The results from the SGM and the WSGGM are always close to the reference.

When the H_2O vapor concentration varies, the absorption coefficient is assumed to be proportional to the concentration in the WSGGM, the gray gas model and the SGM. Figure 6 shows the results for the problem of parabolic H_2O vapor concentration at uniform temperature of 1000 K bounded by cold black walls. The heat source strength of the reference solution shows a W-shaped distribution. The gray gas model does not exhibit this pattern at all. The results of the WSGGM and the SGM show fair agreement with the reference qualitatively and quantitatively as well.

Although not presented in the figures, 2 SGM and 3 SGM have been also tested and they have produced fairly comparable results with the reference. The deviation is slightly larger than that of the 4 SGM, however, they reveal the correct pattern of the curve. Kim *et al.* [15] also presented the gray wide band results which employed the partly gray model around wide band centers as Edwards [7] suggested, and which was also employed by Menguc and Viskanta [13]. The gray wide band results are, in general, worse than other models except the gray gas model. This may be because the gray wide band model is based on the mean beam length at which the modeling is accurate and deteriorating elsewhere. As the last comparison, the wall heat flux at $z = 0$ is given in Table 1. All the available models are compared. The error of the gray gas model is roughly 2–50% depending on the problem. The error is dramatically decreased to 1–11% by 2 SGM. The 3, 4 SGMs and the 4 WSGGM yield as low as 1–10% error. On average, the error in the wall heat flux is less than 5% for all the SGMs and the 4 WSGGM.

The WSGGM does not show significant difference with the SGM in the second type of problems. It is considered that the effect of the last two terms of equation (16) is smeared away in the total spectrum in the WSGGM. Also, the modeling methods of the WSGGM and the SGM are similar to each other, so

Table 1. Net wall heat fluxes (kW m^{-2}) (the wide band data are taken from Kim *et al.* [15])

Problem	Nongray wide band	Gray wide band	Gray gas	2 SGM	3 SGM	4 SGM	4 WSGGM
Parabolic T	−6.6	−8.1	−10.3	−6.0	−7.3	−7.3	−7.0
Uniform T, L = 0.1 m	−14.4	−14.1	−8.7	−14.6	−13.9	−13.7	−14.5
Uniform T, L = 1.0 m	−27.6	−26.3	−42.7	−25.7	−27.8	−28.3	−26.7
Boundary layer T	277.0	281.7	282.4	275.4	275.8	275.7	276.4
Parabolic concentr.	−24.6	−23.6	−35.2	−22.6	−25.4	−25.6	−24.5

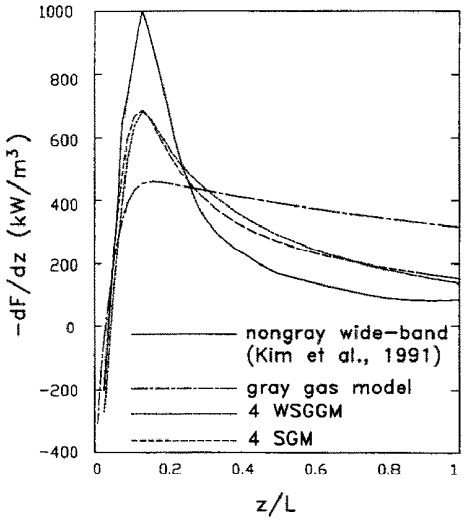

FIG. 5. The radiative source for the boundary layer type temperature of Kim *et al.* [15]. (Temperature: from 1500 K left to 300 K right with black walls of the same boundary temperatures, layer depth = 0.2 m.)

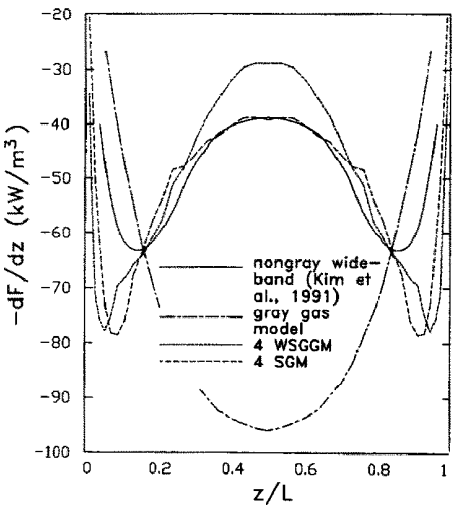

FIG. 6. The radiative source for the parabolic H_2O concentration profile with the uniform temperature profile of Kim *et al.* [15]. (Temperature: 1000 K with cold black walls, concentration: 100% at the center and zero at the boundaries, layer depth = 1.0 m.)

that the results are also expected to be similar to each other. No critical comparison has been made between them since no exact solution is available except for the case of a single line. Either the WSGGM or the SGM may be applied to engineering problems with reliable accuracy. The WSGGM and the SGM are easy to incorporate with any kind of RTE solvers, while the Curtis–Godson approximation or similar methods may be applied to basically ray-tracing techniques such as discrete ordinate method, Monte-Carlo method, etc. The reported CPU time of Kim's nongray wide band computation was about 10 s on a CRAY-2S, while the WSSGM and the SGM computation of heat flux took about 0.5 CPU seconds on a same machine. However, the modeling time of the SGM is about 30 CPU seconds for each number of the spectral groups (the WSGGM takes shorter time). Once the cookbook of the absorption coefficients and the weights is made by the WSGGM or the SGM, the effort is later compensated by the efficiency and versatility of the RTE solution method.

CONCLUSIONS

Two types of problems have been used to examine the validity of the Curtis–Godson approximation, the gray gas model, the WSGGM (Milne–Eddington type), the SGM, the nongray wide band model and the gray wide band model. The commonly employed Curtis–Godson approximation may be erroneous for a single line. Although the Milne–Eddington type WSGGM underestimates the line emission from an inhomogeneous layer of gas, it gives reliable results when applied to the total spectral problems of typical inhomogeneous layer. The WSGGM and the SGM both closely predict the results of the nongray wide band model. The gray gas model and the gray wide band model are not reliable for highly inhomogeneous problems. In the limitation of the problems tested, the WSGGM and the SGM have been proved to meet the criteria of engineering nongray gas modeling on the total spectral basis. More tests are recommended for further verifications.

It is anticipated that a cookbook of the absorption coefficients and the weights using the WSGGM or the SGM will be very useful. When these methods are combined with line-by-line method or the narrow band model, spectral information is also expected to be obtained.

REFERENCES

1. H. C. Hottel and A. F. Sarofim, *Radiative Transfer*, p. 247. McGraw-Hill, New York (1967).
2. T. F. Smith, Z. F. Shen and J. N. Friedman, Evaluation of coefficients for the weighted sum of gray gases model, *ASME J. Heat Transfer* **104,** 602–608 (1982).
3. M. F. Modest, The weighted-sum-of-gray-gases model for arbitrary solution methods in radiative transfer, *ASME J. Heat Transfer* **113,** 650–656 (1991).
4. T. H. Song and R. Viskanta, Development of application of a spectral-group model to radiation heat transfer, *ASME* Paper No. 86-WA/HT-36 (1986).
5. W. L. Grosshandler, Radiative heat transfer in nonhomogeneous gases: a simplified approach, *Int. J. Heat Mass Transfer* **23,** 1447–1459 (1980).
6. C. B. Ludwig, W. Malkmus, J. E. Reardon and J. A. L. Thompson, *Handbook of Infrared Radiation from Combustion Gases*, Chap. 3. NASA SP-3080, Scientific and Technical Information Office, Washington, D.C. (1973).
7. D. K. Edwards, Molecular gas band radiation, *Adv. Heat Transfer* **12,** 115–193 (1976).
8. R. O. Buckius, The effect of molecular gas absorption on radiative heat transfer with scattering, *ASME J. Heat Transfer* **104,** 580–586 (1982).
9. R. M. Goody, *Atmospheric Radiation*. Clarendon Press, Oxford (1964).
10. R. D. Cess and L. S. Wang, A band absorption formulation in non-isothermal gaseous radiation, *Int. J. Heat Mass Transfer* **13,** 547–555 (1970).
11. S. H. Cahn and C. L. Tien, Total band absorptance of non-isothermal infrared-radiating gases, *J. Quant. Spectrosc. Radiat. Transfer* **9,** 1261–1271 (1969).
12. G. H. Lindquist and F. S. Simmons, A band model formulation for very nonuniform path, *J. Quant. Spectrosc. Radiat. Transfer* **12,** 807–820 (1972).
13. M. P. Menguc and R. Viskanta, An assessment of spectral radiative heat transfer predictions for a pulverized coal-fired furnace, *Proceedings of the Eighth Int. Heat Transfer Conference*, San Francisco. Vol. 2, pp. 815–820 (1986).
14. L. Zhang, A. Soufiani and J. Taine, Spectral correlated and noncorrelated radiative transfer in a finite axisymmetric system containing an absorbing and emitting real gas–particle mixture, *Int. J. Heat Mass Transfer* **31,** 2261–2272 (1988).
15. T. K. Kim, J. A. Menart and H. S. Lee, Nongray radiative gas analysis using the S–N discrete ordinates method, *ASME J. Heat Transfer* **113,** 946–952 (1991).
16. J. D. Felske and C. L. Tien, The use of the Milne–Eddington absorption coefficient for radiative heat transfer in combustion systems, *ASME J. Heat Transfer* **99,** 458–465 (1977).
17. J. D. Felske and C. L. Tien, Infrared radiation from non-homogeneous gas mixtures having overlapping bands, *J. Quant. Spectrosc. Radiat. Transfer* **14,** 35–48 (1974).
18. D. A. Nelson, Band radiation of isothermal gases in diffuse-walled enclosures, *Int. J. Heat Mass Transfer* **27,** 1759–1769 (1984).
19. M. N. Ozisik, *Radiative Transfer*, p. 557. Wiley, New York (1973).
20. A. L. Crosbie and R. Viskanta, Effect of band or line shape on the radiative transfer in a nongray planar medium, *J. Quant. Spectrosc. Radiat. Transfer* **10,** 487–509 (1970).